Available online at www.sciencedirect.com

ScienceDirect

Physics Procedia 18 (2011) 222–226

Physics Procedia

The Fourth International Conference on Surface and Interface Science and Engineering

Microstructure and thermal stability of $Ti_{1-x}Al_xN$ coatings deposited by reactive magnetron co-sputtering

Miao Du, Lei Hao*, Xiaopeng Liu, Lijun Jiang, Shumao Wang, Fang Lv, Zhinian Li, Jing Mi

Department of Energy Material & Technology, General Research Institute for Non-ferrous Metals, Beijing 100088, China

Abstract

$Ti_{1-x}Al_xN$ (0.25≤x≤0.75) coatings were deposited by reactive DC/RF magnetron co-sputtering. The phase structure, microstructure, surface roughness and chemical composition were investigated. The anti-oxidation behavior of coatings at high temperature was also studied. It has been shown that the coatings with high Al content (x≥0.67) consisted of hexagonal-AlN and cubic-TiAlN phases, while it has cubic-TiAlN phase for the coatings with low Al content (x<0.67). The roughness of surface of coatings was 1.89~ 4.80nm and it decreased with increasing the Al content. The thermal-stability of the $Ti_{1-x}Al_xN$ coatings increased with increasing Al content.

Selection and/or peer-review under responsibility of Selection and/or peer-review under responsibility of Lanzhou Institute of Physics China

PACS: 65.60 +a; 79.20 Rf

Keywords: $Ti_{1-x}Al_xN$ coating, magnetron co-sputtering, microstructure, thermal stability;

1. Introduction

TiAlN coatings have been attracting more and more attentions since last decade due to their higher oxidation resistance (about 750–800°C), higher hardness (approximately 30-35GPa) and higher corrosion resistance [1]. It had found that the hardness of TiAlN coatings could reach a maximum value of about 40GPa at Al/Ti=1.22 [2]. For this reason, TiAlN coatings have been widely used for cutting tools, especially for dry and high speed machining [3]. TiAlN coatings can also be used as high-density complementary metal-oxide-semiconductor (CMOS) memory devices [4], temperature controlling for the satellite [5], and selective coatings for solar collectors [6-8].

The properties of the TiAlN coatings were considerably related with the Al content and phase structure of coatings [9-11]. In this paper, the phase structure, thermal-stabilization of the $Ti_{1-x}Al_xN$ coatings prepared by reactive DC/RF magnetron co-sputtering was studied.

2. Experimental

$Ti_{1-x}Al_xN$ coatings (x=0.25, 0.33, 0.5, 0.63 and 0.75) were deposited on stainless steel (SS) and Si by reactive DC/RF magnetron co-sputtering using the metallic titanium (99.5%) and aluminum (99.5%) targets under $Ar+N_2$ plasma. The Ti and Al targets were powered by direct current (DC) and radio frequency (RF) magnetron sputtering, respectively. Before putting the substrates into the vacuum chamber the substrates were mechanical polished and chemically cleaned in an ultrasonic agitator in acetone and absolute alcohol. The vacuum chamber was pump down to a base pressure of 5.0×10^{-3}Pa. The pumping system consisted of a molecular pump backed by a mechanical pump. Subsequently, the substrates were cleaned by argon ion bombardment for 10 min, wherein a DC bias of -600 V was applied to the substrate at an argon pressure of 1.0Pa. The deposition was carried out at room temperature and the substrate was rotated regularly with 1 rpm during the deposition. The base and sputtering vacuum were 5.0×10^{-3}Pa and 0.85Pa, respectively. The substrate bias was -80V. The expected Al/Ti atoms ratio of Ti_{1-}

1875-3892
Selection and/or peer-review under responsibility of Selection and/or peer-review under responsibility of Lanzhou Institute of Physics, China.
doi:10.1016/j.phpro.2011.06.085

$_xAl_xN$ coatings was adjusted by DC and RF power. The sputtering parameters were summarized in Table 1. The coatings were annealed at 700°C for 2.5h in air to study the thermal-stability characteristic.

Table 1 Sputtering parameters for $Ti_{1-x}Al_xN$ coatings

Samples	DC power（W）	RF power（W）	x
1	1050	600	0.25
2	875	600	0.37
3	700	600	0.50
4	700	900	0.67
5	350	900	0.75

Crystal structure was measured by X-ray diffraction using Philips X'Pert Pro with Cu K α radiation. The micrograph and chemical compositions were observed by field emission scanning electron micrographs using Hitachi model S4800 with an energy dispersive X-ray spectrometer (EDX). Roughness of surface was measured by using atomic force microscopy (AFM, Digital Instruments Nanoscope III).

3. Results and discussion

3.1. Phase structure

Fig 1 shows the XRD patterns of the $Ti_{1-x}Al_xN$ coatings. One can see that the coatings with low Al content (x=0.25, 0.37 and 0.5) consist of a major cubic (Ti, Al) N phase. The increase of 2θ values of main peaks reveals that the lattice parameters of the (Ti, Al) N phase decrease with increasing the Al addition content, this is caused by smaller Al atoms replacing some Ti atoms in the cubic-TiN lattice. The coatings with high Al content (x=0.67 and 0.75) consist of hexagonal-AlN and cubic-TiAlN phases, indicating that Al begins to combine with N_2 to form AlN when x>0.67. Min Zhou et al. [12] reported the similar results in the phase transformation between B1 (TiN) and B4 (AlN) in the Ti-Al-N system. When Al content attains x=0.67, intensity of (111) and (200) peaks decreases. The decrease of intensity indicates that crystallization is reduced by lattice defects.

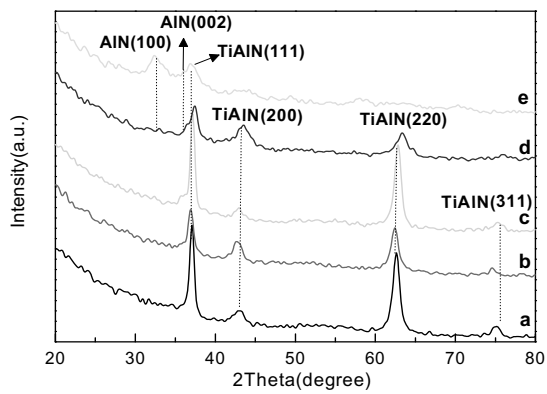

Fig.1 XRD patterns of $Ti_{1-x}Al_xN$ coatings (a) $Ti_{75}Al_{25}N$ (b) $Ti_{63}Al_{37}N$ (c) $Ti_{50}Al_{50}N$ (d) $Ti_{33}Al_{67}N$ (e) $Ti_{25}Al_{75}N$

3.2. Morphology

Fig.2 shows the surface scanning electron micrographs of $Ti_{1-x}Al_xN$ coatings. The coatings of $Ti_{75}Al_{25}N$ (Fig. 2a), $Ti_{63}Al_{37}N$ (Fig. 2b) and $Ti_{50}Al_{50}N$ (Fig.2c) exhibit the pyramid-like structure, which are attributed to the preferred growth along (220) and (111) direction. However in the case of $Ti_{33}Al_{67}N$ (Fig. 2d) and $Ti_{25}Al_{75}N$ (Fig. 2e) coatings don't show the pyramid-like grains, because excessive AlN hinders the preferred growth of the coatings and induces the phase separation which is also indicated in the XRD patterns. And it can be noticed that the surface became more compact and denser with increasing the Al/Ti ratio.

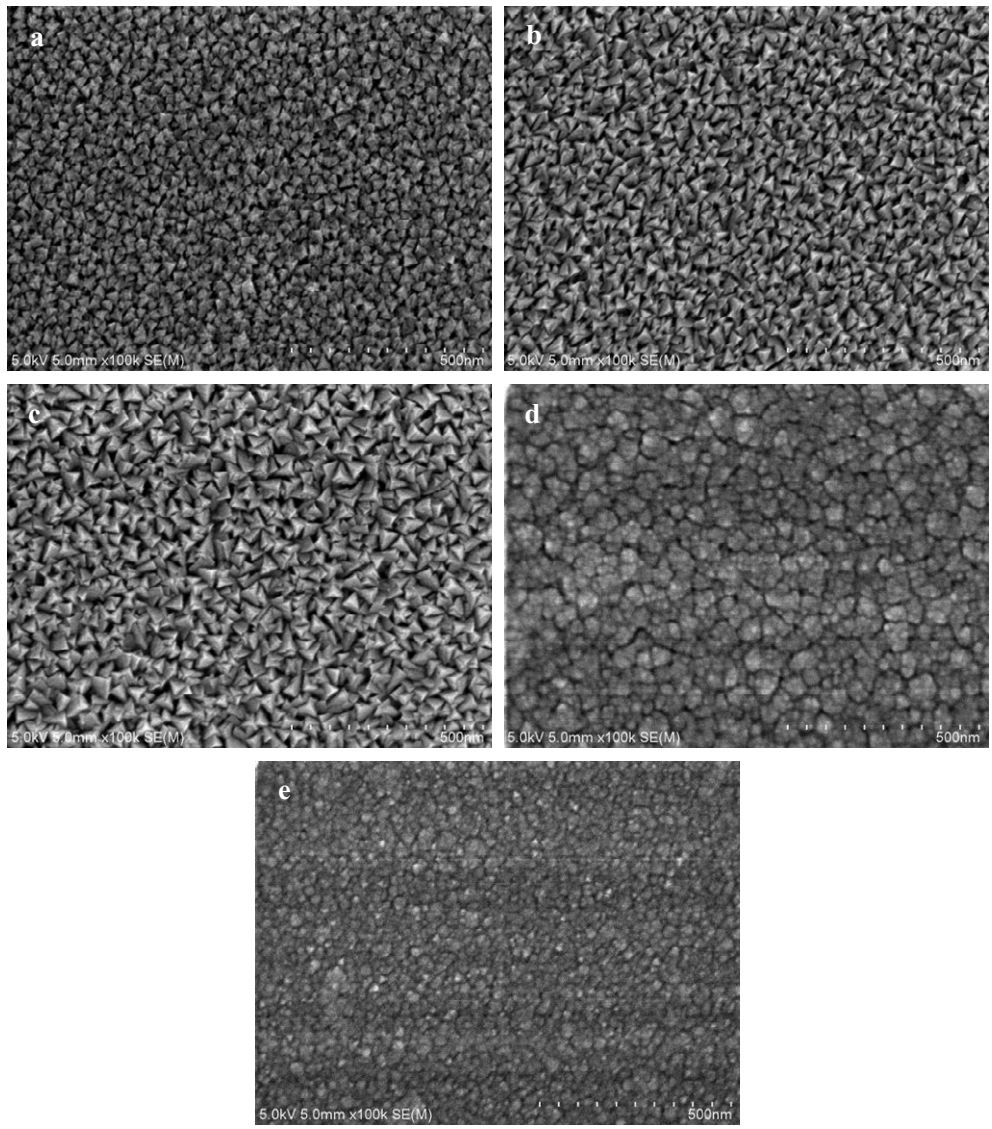

Fig.2 Scanning electron micrographs of $Ti_{1-x}Al_xN$ coatings (a) $Ti_{75}Al_{25}N$ (b) $Ti_{63}Al_{37}N$ (c) $Ti_{50}Al_{50}N$ (d) $Ti_{33}Al_{67}N$ (e) $Ti_{25}Al_{75}N$

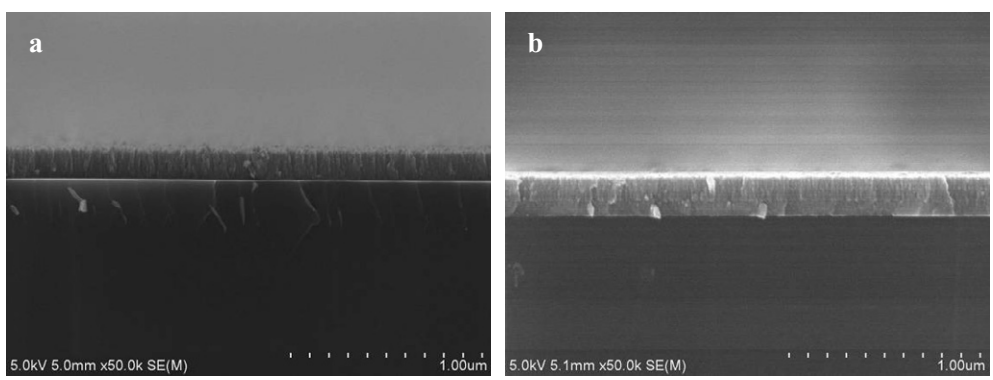

Fig.3 Cross-section morphology of $Ti_{1-x}Al_xN$ coatings (a) $Ti_{75}Al_{25}N$ (b) $Ti_{25}Al_{75}N$

The cross-section micrographs of $Ti_{75}Al_{25}N$ (Fig. 3a) and $Ti_{25}Al_{75}N$ (Fig. 3b) coatings are shown in Fig. 3. The coatings exhibit columnar morphology along the vertical direction of substrate. The other coatings have the similar columnar morphology, so they are omitted. But it should be noted that the column texture in the $Ti_{1-x}Al_xN$ coatings becomes ambiguous with increasing Al content. The column diameter of $Ti_{25}Al_{75}N$ coating is about 20~30nm, which is finer than that of $Ti_{75}Al_{25}N$ coating. J. Wagner et al. [13] reported the similar results showing that TiAlN coatings deposited by thermal CVD had the finer grain size with increasing the Al contents. Since it is known that increase of Al contents results in the coatings having a compositional defects through transformation to metastable phase and finer grain size due to decrease of grain boundary mobility[14].

The roughness of surface of the coatings is shown in Fig.4. The surfaces are considerably smooth and the root mean square (RMS) roughness of the surface are 4.88 nm, 3.98 nm, 3.27 nm, 2.41 nm and 1.89nm for the $Ti_{1-x}Al_xN$ coating with x=0.25, 0.37, 0.5, 0.67 and 0.75, respectively. The decrease of roughness with increasing Al content is attributed to the fact that the coatings prepared at a higher Al content gives a denser and compacter morphology compared with that prepared with a lower Al content, as is evident from the SEM micrographs.

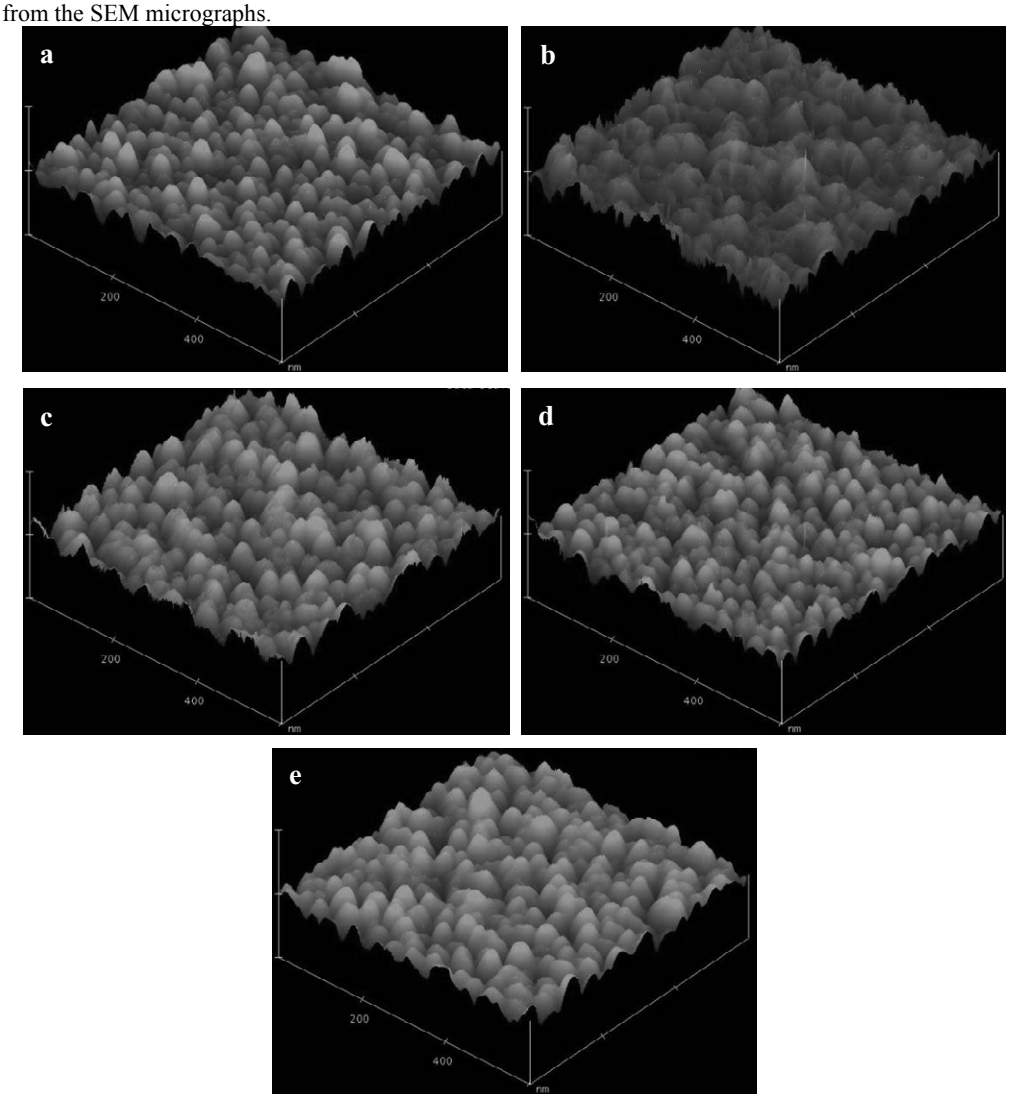

Fig.4 Three-dimensional images of $Ti_{1-x}Al_xN$ coatings (a) $Ti_{75}Al_{25}N$ (b) $Ti_{63}Al_{37}N$ (c) $Ti_{50}Al_{50}N$ (d) $Ti_{33}Al_{67}N$ (e) $Ti_{25}Al_{75}N$

3.3. Thermal stability

In order to study the oxidation resistance behavior of $Ti_{1-x}Al_xN$ coatings, the samples deposited on Si substrates were annealed at 700°C for 2.5h in air atmosphere. The XRD patterns of as-annealed samples are shown in Fig.5. Compared with as-deposited films, the peaks attributed to TiO_2, Al_2O_3 and TiAlN phases are observed in the as-annealed samples, which indicated that $Ti_{1-x}Al_xN$ was partially oxidized at 700°C. Furthermore, one can see that Ti-rich $Ti_{75}Al_{25}N$ coating consists of a major TiO_2 phase with rutile type structure, but the Al-rich $Ti_{33}Al_{67}N$ and $Ti_{25}Al_{75}N$ coatings consist of major Al_2O_3 phase.

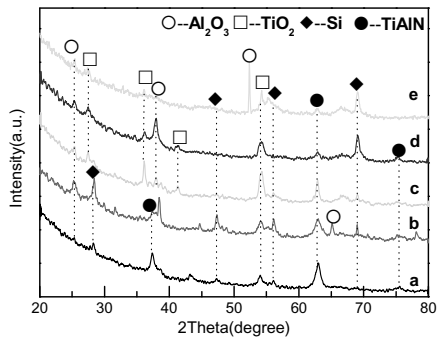

Fig.5 XRD patterns of $Ti_{1-x}Al_xN$ coatings annealed at 700°C in air for 2.5h (a) $Ti_{75}Al_{25}N$ (b) $Ti_{63}Al_{37}N$ (c) $Ti_{50}Al_{50}N$ (d) $Ti_{33}Al_{67}N$ (e) $Ti_{25}Al_{75}N$

It is reported that the aluminum composition in the coatings is attributable to form the Al_2O_3 layer on the coating surface, which is helpful to prevent the oxygen to go deep into specimen as temperature is increasing to a higher stage [15]. So it is reasonable to deduce that $Ti_{1-x}Al_xN$ coating with high Al content have better oxidation resistance than those with low Al content.

4. Conclusions

$Ti_{1-x}Al_xN$ ($0.25 \le x \le 0.75$) coatings were deposited by reactive DC/RF magnetron co-sputtering. The coatings deposited with high Al content ($x \ge 0.67$) consist of hexagonal-AlN and cubic-TiAlN phases, while the coatings with low Al content ($x < 0.67$) has major cubic-TiAlN phase. The coatings have a columnar morphology along the vertical direction of the substrate. As Al content in the $Ti_{1-x}Al_xN$ coating increased, the roughness of coating's surface decreases and columnar texture becomes ambiguous. $Ti_{1-x}Al_xN$ coating with high Al content has better thermal stability than that of coating with low Al content.

References

1. Munz W D. Titanium aluminum nitride films: A new alternative to TiN coatings. J. Vac. Sci. Technol. 4 (1986) 2717-2725.
2. Ding X Z, Bui C T, Zeng X T. Abrasive wear resistance of $Ti_{1-x}Al_xN$ hard coatings deposited by a vacuum arc system with lateral rotating cathodes. Surf. Coat. Technol. 203 (2008) 680-684.
3. J.C. Oliveira, A. Manaia, A. Cavaleiro. Hard amorrphous Ti-Al-N coatings deposited by sputtering. Thin Solid Films 516 (2008) 5032-5038.
4. D.G. Park, T.H. Cha, S.H. Lee, I.S. Yeo. Characteristics of sputtered $Ti_{1-x}Al_xN$ films for storage node electrode barriers. J. Vac. Sci. Technol. 19(6) (2001) 2289-2294.
5. J.T. Chen, J. Wang, F. Zhang, G.A. Zhang, X.Y. Fan, Z.G. Wu, P.X. Yan. Characterization and temperature controlling property of TiAlN coatings deposited by reactive magnetron co-sputtering. J. Alloys compd. 472 (2009) 91-96.
6. H.C. Barshilia, N. Selvakumar, K.S. Rajam. TiAlN/TiAlON/Si_3N_4 tandem absorber for high temperature solar selective applications. Appl. Phys. Lett. 89. 191909 (2006).
7. A. Biswas, D. Bhattacharyys, H.C. Barshilia, N. Selvakumar, K.S. Tajam. Spectroscopic ellipsometric characterization of TiAlN/TiAlON/Si_3N_4 tandem absorber for solar selective applications. Appl. Surf. Sci. 254 (2008) 1694-1699.
8. H.C. Barshilia, N. Selvakumar, K.S. Rajam, A. Biswas. Optical properties and thermal stability of TiAlN/AlON tandem absorber prepared by reactive DC/RF magnetron sputtering. Sol. Energy Mater. Sol. Cells 92 (2008) 1425-1433.
9. J. Bujak, J. Walkowicz, J. Kusinski. Influence of the nitrogen pressure on the structure and properties of (Ti, Al) N coatings deposited by cathodic vacuum arc PVD process. Surf. Coat. Technol. 180-181 (2004) 150-157.
10. K. Chakrabarti, J.J. Jeong, S.K. Hwang, Y.C. Yoo, C.M. Lee. Effects of nitrogen flow rates on the growth morphology of TiAlN films prepared by an rf-reactive sputtering technique. Thin Solid Films 406 (2002) 159-163.
11. J.H. Hsieh, C. Liang, C.H. Yu, W. Wu. Deposition and characterization of TiAlN and multi-layered TiN/TiAlN coatings using unbalanced magnetron sputtering. Surf. Coat. Technol. 108-109 (1998) 132-137.
12. Min Zhou, Y. Makion, M. Nose, K. Nogi. Phase transition and properties of Ti-Al-N thin films prepared by r.f.-plasma assisted magnetron sputtering. Thin Solid Films 339 (1999) 203-208.
13. J. Wagner, V. Edlmayr, M. Penoy, C. Michotte. Deposition of Ti-Al-N coatings by thermal CVD. Int. J. Refract. Met. Hard mater.s 26 (2008) 563-568.
14. Sang Shik Park, Soon Gil Yoon. High temperature oxidation of TiAlN thin films for memory devices. Integr. Ferroelectr. 48 (2002) 281-290.
15. Ming Sheng Leu, Shen Chuan Lo, Jin Bao Wu, Ai Kang Li. Microsuructure and physical properties of arc ion plated TiAlN/Cu thin film. Surf. Coat. Technol. 201 (2006) 3982-3986.